

# Lattice Design Principles for a Recirculated, High Energy, SRF Electron Accelerator\*

0205 9100 004 432 4

David R. Douglas  
Continuous Electron Beam Accelerator Facility  
12000 Jefferson Avenue,  
Newport News, Va. 23606

## Abstract

Issues critical to the design of a high energy (over 10 GeV), recirculated, superconducting RF (SRF) based electron accelerator are discussed. These include injection energy, number of passes, type of linac focussing structure (constant gradient or constant focal length), quantum excitation in recirculation arcs, method of beam separation for recirculation, and use of isochronous or nonisochronous transport. An example lattice for a 16 GeV SRF linac with a CEBAF-like footprint is presented.

## I. INTRODUCTION

This paper will discuss lattice issues relevant to the design of the CEBAF 4 GeV SRF electron accelerator [1], and extrapolate to determine their interactions and impact on a high energy (> 10 GeV or higher) multipass electron linac based on SRF technology. An example lattice, for a 16 GeV linac with a CEBAF-like footprint, is given.

## II. FUNDAMENTAL DESIGN ISSUES

Several technical issues have arisen during the design of the CEBAF 4 GeV linac. Their impact in that context has been discussed elsewhere [2]. We now examine how they influence the design of a linac of final energy of over 10 GeV.

Certain features are assumed common to all designs. The machine will comprise an injector, multiply recirculated superconducting linac(s), and a recirculator. The recirculator will either commonly transport beams at multiple energies, or will have individual beam lines transporting monoenergetic beams, using a "spreader" to separate the beams for transport following the linac(s), and a "recombiner" to combine them for reinjection.

The intent of any design is to produce a lattice supporting specific performance goals. In the following, we attempt to achieve electron beam currents of 10–100  $\mu\text{A}$  with  $E_{\text{final}} > 10$  GeV, beam emittances  $\epsilon_{\text{rms}} < 10$  nm-rad, and energy spread  $\sigma_{\Delta E/E} < 2.5 \times 10^{-4}$ . A desire for minimum cost, easy operability, and upgradability is assumed. SRF technology is adopted as the preferred method to achieve high duty factor and superior beam quality.

### A. Injection Energy

Injection energy is primarily cost limited. Higher values provide better performance, by reducing peak betatron envelope values in multiple passes; higher front end linac energy has associated with it higher focussing strength. For example, the peak betatron function values in the four pass 4 GeV CEBAF design (45 MeV at injection) were over 200 m in  $x$  and  $y$  [3]. In an optically identical 16 GeV linac design discussed below (1 GeV at injection), the peak betatron function values are only about 130 m in  $x$  and  $y$ . This stronger focussing also provides greater stability

against multipass beam breakup. It enhances ease of operation, by lowering error sensitivity due to pass-to-pass betatron mismatch. Finally, use of high injection energy and a short linac (low single pass linac energy gain) may allow use of low linac focussing (e.g. quadrupole excitations at constant gradient, instead of constant focal length). This simplifies pass-to-pass betatron matching of the recirculation transport system.

### B. Number of Passes, $N_{\text{pass}}$

To first order, this is a cost optimization issue: trade linac cost ( $\propto 1/N_{\text{pass}}$ ) off against recirculator costs ( $\propto N_{\text{pass}}$ ), and seek the cost minimum.

Higher order effects may be significant. As  $N_{\text{pass}}$  increases, mechanical and operational complexity of the recirculator (in particular, the spreaders and recombiners) increases, driving costs up at a rate  $\propto N_{\text{pass}}^2$  or higher. The choice of single vs. split linac can affect cost in an  $N_{\text{pass}}$ -dependent manner. A split linac is relatively more complex than a single linac; in the limit of a short linac and many passes the split linac will have higher costs (due to the need for two spreader/recombiner pairs per pass).

Betatron mismatch and error sensitivity increase with  $N_{\text{pass}}$ , the former due to lowered first pass linac focussing, the latter due to increased total beam path length. Both cause an increase in operational complexity and a decrease in machine performance.

### C. Single vs. Split Linac

A split linac is an effective use of tunnel length and minimizes the cost of unit acceleration per unit tunnel length. However, the cost and performance optimum for a given machine also depends on the type of beam transport used for recirculation and the number of passes. A highly modular, many pass transport system requires relatively complex spreaders and recombiners; tunnel cost savings achieved by using a split linac could be offset by the incremental cost of the additional required spreader/recombiner pair. The use of a split linac also entails some operational complexity as the number of betatron phase space matches of recirculator transport to linac and the number of linac reinjections is doubled, as is the number of adjustments of beam path length to match the beam to linac accelerating phase.

Certain designs are not amenable to split or multiple linacs. Microtron-like recirculators are most easily designed for a single linac; use of multiple linacs can force utilization of complex magnetic components with severe error tolerances. Finally, a machine may be site-limited to the choice of either single or split linac; in particular, a short, wider, site will favor the use of a split linac.

### D. Type of Linac Focussing Structure

Linac focussing structure can be either constant gradient focussing (which has zero gradient—no focussing—as a sub-case), or focussing varying in gradient along the linac (typically, constant focal length focussing).

\*Supported by D.O.E. contract #DE-AC05-84ER40150

Constant gradient allows simple optical matching for multi-pass operation. However, the maximum focussing strength is set by transverse (betatron) stability of the injected beam, and is thus limited by injection energy. On higher energy passes, the linac will appear more and more "drift-like"; the maximum betatron excursion is thus dictated by the linac length. This type of focussing is therefore best suited to a machine with short linac(s) and high injection energy, such as a cascaded microtron.

In constant focal length optics, focussing along the linac is limited by betatron stability of the first pass; thus, on higher passes, the beam experiences more focussing in the back end of the linac than it would with constant gradient focussing. This "back-end focussing" can, with proper choice of reinjection condition, compensate for lack of focussing of recirculated beams, and provide greater betatron stability than constant gradient focussing. Constant focal length optics are thus well suited for use in a long linac with low injection energy. If the injection energy is raised, the performance improves (as in constant gradient focussing).

A comparison of these focussing methods for a 16 GeV machine described below is given in Table 1, in which peak beta functions and total phase advance through a four pass linac are tabulated. The linac comprises 50 cryomodules embedded in 19.2 m long FODO cells; the first linac quad is set to give 120° phase advance per cell on the first pass. Constant focal length focussing provides about 50% lower peak envelope functions, and much higher total phase advance, than does constant gradient, for the specified front-end FODO cell betatron tune.

Table 1  
Comparison of Focussing Structures for 16 GeV Linac

Pass	Constant Gradient				Constant Focal Length			
	$\beta_x$ (m)	$\psi_x$	$\beta_y$ (m)	$\psi_y$	$\beta_x$ (m)	$\psi_x$	$\beta_y$ (m)	$\psi_y$
1	82	3.00	63	3.02	41	8.34	41	8.34
2	99	1.08	99	1.08	62	2.97	85	2.98
3	143	0.68	149	0.69	98	1.85	93	1.88
4	193	0.49	199	0.49	132	1.34	121	1.37

#### E. Degree of Functional Modularity

It is important to specify the degree of functional modularity to be employed. In the limit of nonmodularity, a microtron-like machine could be designed, in which recirculated beams of all energies are transported by a common (set of) dipole(s). Toward the limit of higher modularity, accelerated beams of various energies could be separated for recirculation by individual transport channels. Given this, a second level of modularity must be set, in which various transport functions of the mono-energetic beam lines are accomplished either globally, or locally, in a modular fashion. The CEBAF 4 GeV accelerator [4] is an example of a modular transport system, in which only a few parameters are coupled to any particular control variable.

Modularity trades construction costs off against operational costs, flexibility, and upgradability. Modular systems generally require more parts than nonmodular systems. They therefore may have higher construction costs, though the complexity of components for nonmodular systems can reduce the cost differential. However, modular transport allows use of simple tuning algorithms and provides operational flexibility absent in nonmodular recirculators. (See the following discussion of isochronous vs. non-isochronous transport.)

#### F. Quantum Excitation in Recirculator Arcs

Emitance and momentum spread growth from quantum excitation can be estimated [5]. The absolute energy spread,  $\sigma_E^2$ , and the emittance,  $\Delta\epsilon$ , generated by bending a monoenergetic, zero emittance beam through 180° are

$$\sigma_E^2 = 1.18 \times 10^{-33} \text{ GeV}^2 \text{ m}^2 \frac{\gamma^7}{\rho^2}$$

$$\Delta\epsilon = 7.19\pi \times 10^{-28} \text{ m}^2 \text{ rad} \frac{\gamma^5}{\rho^2} \langle \mathcal{H} \rangle,$$

$$\langle \mathcal{H} \rangle = \left( \frac{1}{L} \right) \int_{\text{bends}} ds \left\{ \left( \frac{1}{\beta} \right) [\eta^2 + (\beta\eta' - \frac{1}{2}\beta'\eta)^2] \right\},$$

where  $L$  = orbit length, and  $\rho$  = orbit radius, in bends.

At a given energy,  $\sigma_E^2$  is a function of  $\rho$  only;  $\Delta\epsilon$  is a function of both  $\rho$  and  $\langle \mathcal{H} \rangle$ . Thus, bend radii are limited by the final momentum spread specification; betatron parameters are then optimized to control emittance. It is particularly useful to keep dispersion,  $\eta$ , small in the dipoles. This is readily achieved if achromatic, isochronous transport is invoked.

#### G. Method of Beam Separation for Recirculation

Assuming use of modular transport, a mechanism for separation or recombination of the multiple energy beams on the linac axis (axes) is needed. Small, recirculated single linacs may easily separate beams in the plane of recirculation. High energy machines are, however, constrained by tunnel size. It is then best to separate out of the recirculation plane, so that the various energy-specific beam lines can be stacked vertically. They are then presented for easy installation and maintenance.

The separation of beams will generate transverse dispersion. Control of this dispersion is desirable to limit quantum excitation. If the separation is in the recirculation plane, dispersion may be suppressed locally (in the spreader itself), or matched to the dispersion inherently present in the recirculator. If spreading is out of the recirculation plane, dispersion can be locally suppressed, or mapped to the recirculation plane through the use of a skew-quad rotator, and matched to the recirculator dispersion. The latter entails significant operational complexity.

There are several modular methods of dispersion suppression. In the CEBAF 4 GeV design, two methods were examined: a simple achromatic transverse (vertical) translation [6], which was rejected because of high error sensitivity generated by strong focussing, and a "staircase" (vertical) spreader [7], which has been built. Although optically superior, the staircase suffers from some mechanical complexity due to congestion of transport elements immediately following the linac. In a following section, we describe an asymmetric chicane based spreader, which lacks some optical symmetries of other solutions, but avoids component congestion and seems to have low error sensitivity.

#### H. Use of Isochronous vs. Nonisochronous Transport

In non-modular systems there is typically little tuning range for momentum compaction. It is set by the geometry of the transport. Careful consideration of the use of nonisochronous transport vs. isochronous transport is therefore needed at the design stage.

Functionally modular transport systems have demonstrably tunable momentum compaction [8]. Therefore, no

design decision is required; momentum compaction can be adjusted to meet operational needs.

### I. Error Sensitivity

Error sensitivities must be considered in all design choices. They tend to grow as the square root of number of machine elements and/or machine length, for uncorrelated errors, and linearly in number of elements and/or machine length, for correlated errors. In addition, sensitivity is greater in designs with greater betatron mismatch. It therefore interacts with the number of passes, the type of linac focussing, injection energy, use of a single or split linac, and degree of functional modularity.

An analysis of error sensitivities should be conducted for any particular design. Appropriate design modifications must then be made, and error analyses iterated.

### III. A 16 GEV SRF LINAC

The following design is an exercise promulgated on two assumptions. First, the following example of a 16 GeV machine will fit on a CEBAF-sized site. Secondly, it is assumed that currently available gradients in CEBAF SRF cavities [9] continue to rise to  $\sim 20$  MV/m. The target beam performance for the design is as discussed above.

Injection energy is selected to be 1 GeV, to reduce the injection-to-final-energy ratio of the machine from the current CEBAF value of 90 to 1 to the level of 16 to 1. The advantages of this are discussed above.

It is assumed that SRF production costs rise only modestly in going to 20 MV/m, while beam transport costs increase significantly in going from 4 to 16 GeV final energy. The optimum number of passes will therefore fall; we choose four passes as a design value. We are site constrained to a split linac. The data of Table 1 suggest that constant focal length linac focussing is to be desired; we duplicate the present CEBAF linac focussing structure of 12 1/2 120° FODO cells in each linac. The resulting linacs use 25 eight cavity cryomodules, with each cavity supplying 9.375 MeV energy gain, for a single pass energy gain of 3.75 GeV.

A high degree of functional modularity is preferred operationally. Beams are separated vertically for recirculation using a spreader based on a dispersion-suppressed asymmetric chicane. This is depicted in Figure 1. Beam recombination and reinjection matching occur as in a time-reversed propagation through the spreader.

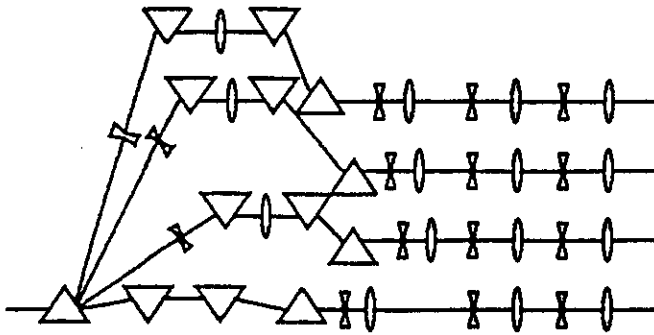


Figure 1. Schematic of spreader/recombiner.

Preliminary computations suggest dispersion suppression and matching of linac beam envelope functions to arc acceptance require modest quadrupole strengths and generate little betatron mismatch. Error sensitivity will therefore be low.

The seven recirculation arcs proper are configured to provide large bend radius (to control energy spread generation) and strong focussing (to limit emittance excitation). Initial studies indicate that combined function dipoles are required to limit quantum excitation of emittance. Each arc consists of six superperiods of the following "six-cell" alternating gradient focussing structure.

$$\frac{1}{2}\text{QD1-BF-BD-QF-BD-BF-QD2-BF-BD-QF-BD-BF}-\frac{1}{2}\text{QD1}$$

Each superperiod is tuned to 7/6 wavelength horizontally and 5/6 wavelength vertically. The resulting arc is thus a second order achromat. Three quadrupole families allow operational control of tunes and momentum compaction. (Dipole field indices are selected to give small superperiod matched dispersion for isochronous arc transport and to allow for a broad tuning range on momentum compaction.) On the final pass, for isochronous transport, net relative energy spread excitation is  $\sigma_{\Delta E/E} = 1.6 \times 10^{-4}$ , quantum excitation is specified by  $\langle \mathcal{H} \rangle = 0.167$  m, and net emittance excitation is  $\Delta \epsilon_x = 2.1 \times 10^{-9}$  m-rad. Relevant magnetic parameters are summarized in Table 2.

Table 2: Arc Transport System Parameters for 16 GeV Recirculator

Global focussing structure	2nd order achromat
Superperiodicity	6
Superperiod focussing structure	6 "cell" a - g
#dipoles	48
Bend radius (m)	53.476
Bend index, $n = -(\rho/B)\partial B/\partial x$	-310.56
Bend magnetic length (m)	3.5
Peak bend field (kG)	8.811
Minimum quadrupole focal length (m)	1.39
Superperiod phase advance, $\psi_{x,y}$	$2\pi \times 7/6, 5/6$
$M_{56}$ range (m)	$ M_{56}  < 1$
Superperiod matched $\beta_{x,y}$ (m), ( $M_{56} = 0$ )	29.58, 31.47
Superperiod matched $\eta_x$ (m), ( $M_{56} = 0$ )	0.17
Superperiod $\partial \nu_{x,y}/\partial \delta$ , ( $M_{56} = 0$ )	-3.02, -1.43

### IV. ACKNOWLEDGMENTS

I would like to thank Joseph Bisognano, Nathan Isgur, Leigh Harwood, and Christoph Leemann for many useful discussions on this topic.

### V. REFERENCES

- [1] B. Bowling *et al.*, "The CEBAF Beam Transport System Lattice Design," *Proc. 1991 IEEE Part. Acc. Conf.*, San Francisco, CA, May, 1991, pp. 446-448.
- [2] *ibid.*
- [3] R. C. York and D. R. Douglas, "Optics of the CEBAF CW Superconducting Accelerator," *Proc. 1987 IEEE Part. Acc. Conf.*, Washington, D.C., March, 1987, pp. 1292-1294.
- [4] B. Bowling, *op. cit.*
- [5] R. C. York and D. R. Douglas, *op. cit.*; M. Sands, "Emittance Growth From Radiation Fluctuations", SLAC Report SLAC/AP-47, Dec., 1985.
- [6] R. C. York and D. R. Douglas, *op. cit.*
- [7] D. R. Douglas *et al.*, "Optical Design of the CEBAF Beam Transport System," *Proc. 1989 IEEE Part. Acc. Conf.*, Chicago, IL, March, 1989, pp. 557-559.
- [8] Y. Chao *et al.*, "Commissioning and Operation Experience With the CEBAF Recirculation Arc Beam Transport System", these proceedings.
- [9] F. Dylla, "Operating Experience with SRF Cavities", these proceedings.